*Cerebral Cortex*, 2018; 1–11

**doi: 10.1093/cercor/bhy268**
Original Article

ORIGINAL ARTICLE

# High-Expanding Regions in Primate Cortical Brain Evolution Support Supramodal Cognitive Flexibility

Markus H. Sneve [1], Håkon Grydeland [1], Marcello G.P. Rosa [2,3,4], Tomáš Paus[5,6,7,8], Tristan Chaplin[2,3,4], Kristine Walhovd[1,9] and Anders M. Fjell [1,9]

[1]Center for Lifespan Changes in Brain and Cognition, Department of Psychology, University of Oslo, Oslo, Norway, [2]Department of Physiology, Monash University, Clayton, VIC 3168, Australia, [3]Biomedicine Discovery Institute, Monash University, Clayton, VIC 3168, Australia, [4]Australian Research Council, Centre for Excellence for Integrative Brain Function, Monash University, Clayton, VIC 3168, Australia, [5]Rotman Research Institute, University of Toronto, Toronto, Canada M6A 2E1, [6]Department of Psychiatry, University of Toronto, Toronto, Canada M5S 1A1, [7]Center for Developing Brain, Child Mind Institute, New York, NY 10022, USA, [8]Department of Psychology, University of Toronto, Toronto, Canada M5S 1A1 and [9]Department of Radiology and Nuclear Medicine, Oslo University Hospital, Oslo, Norway

Address correspondence to Markus Handal Sneve, Department of Psychology, Pb. 1094 Blindern, 0317 Oslo, Norway. Email: m.h.sneve@psykologi.uio.no orcid.org/0000-0001-7644-7915

## Abstract

Primate cortical evolution has been characterized by massive and disproportionate expansion of a set of specific regions in the neocortex. The associated increase in neocortical neurons comes with a high metabolic cost, thus the functions served by these regions must have conferred significant evolutionary advantage. In the present series of analyses, we show that evolutionary high-expanding cortex – as estimated from patterns of surface growth from several primate species – shares functional connections with different brain networks in a context-dependent manner. Specifically, we demonstrate that high-expanding cortex is characterized by high internetwork functional connectivity; is recruited flexibly over many different cognitive tasks; and changes its functional coupling pattern between rest and a multimodal task-state. The capacity of high-expanding cortex to connect flexibly with various specialized brain networks depending on particular cognitive requirements suggests that its selective growth and sustainment in evolution may have been linked to an involvement in supramodal cognition. In accordance with an evolutionary-developmental view, we find that this observed ability of high-expanding regions – to flexibly modulate functional connections as a function of cognitive state – emerges gradually through childhood, with a prolonged developmental trajectory plateauing in young adulthood.

**Key words:** cerebral cortex, functional connectivity, human brain evolution, human development, multimodal integration

## Introduction

The most striking feature of the human brain when compared with brains of other primates, is its massively expanded cerebral cortex, mainly due to a higher number of cortical neurons (Herculano-Houzel 2012; Buckner and Krienen 2013). The growth of the primate cortex has not been uniform, however, with a set of so-called "hotspot" regions in lateral temporal, parietal and prefrontal cortex showing disproportionally high

expansion (Hill et al. 2010; Chaplin et al. 2013). Well-supported models suggest that this non-uniform growth has followed allometric scaling laws, and that the massive expansion of certain regions in evolution therefore is a predicted consequence of growing a bigger brain (Finlay and Darlington 1995; Toro et al. 2008; Herculano-Houzel 2012; Chaplin et al. 2013; Rilling 2014; Amlien et al. 2016; although see e.g., Smaers et al. 2017). Nevertheless, the metabolic costs associated with sustaining a higher number of neurons are high (Ringo 1991; Herculano-Houzel 2011) and impose limitations on the growth of other, non-neuronal, physical capacities such as body size (Fonseca-Azevedo and Herculano-Houzel 2012). An intriguing question is therefore: what functions do high-expanding regions in primate brain evolution serve, which may have offset these potential natural selection costs?

Expansion "hotspots" refer to the cortical regions that differ the most between extant primates of different brain sizes (Chaplin et al. 2013) and are considered a useful proxy for the parts of cortex that have undergone the most expansion during evolution (Hill et al. 2010; Buckner and Krienen 2013). As prototypical members of association cortex, these evolutionary high-expanding regions are involved in various tasks and functional systems and have been theorized to serve relational reasoning and integrative higher-order cognition (Krienen et al. 2014; Vendetti and Bunge 2014). In support of these views, measures of general cognitive abilities in human adults have been shown to correlate positively with cortical surface-area within high-expanding regions (Fjell et al. 2015), associations not found within low-expanding cortex (Vuoksimaa et al. 2016). Furthermore, when compared with brain regions showing less evolutionary expansion, high-expanding cortex shows higher growth of the surface area during human development (Hill et al. 2010; Amlien et al. 2016), and this pattern is more pronounced in individuals with high intelligence (Schnack et al. 2015).

In the current study, we tested the hypothesis that the growth and sustainment of high-expanding cortex has facilitated supramodal cognition (Goldman-Rakic 1988), conceptualized as the integration of information from across the brain in a flexible manner. By taking advantage of recent developments in brain network analysis (Rubinov and Sporns 2010), and applying these to histological data and magnetic resonance imaging (MRI) scans of multiple primate brains, as well as a large sample of humans during different cognitive states and at different stages in development, we were able to directly test the predictions that high-expanding cortex (1) has broad functional connections with different specialized brain networks; (2) is flexibly engaged by a diverse set of cognitive tasks; (3) is more central to communication flow in the brain during states requiring multimodal integration than during low-demand states; and (4) increases functional coupling preferentially with regions engaged by the current cognitive demands. Moreover, given the correlation between morphological changes in primate brain evolution and human development, we predict that the functional connectivity patterns associated with supramodal cognition develop gradually, and fully emerge relatively late in postnatal life.

## Materials and Methods

### Human Subjects

RsfMRI-data were collected in 221 healthy young adults (age range 18–38, mean age 23.8; 142 females). Task-fMRI data were collected in 105 of the same participants (age range 18–38, mean age 25.3; 69 females), as well as in 46 children and adolescents (age range 6–17, mean age 12.9; 21 females). The study was approved by the Regional Ethical Committee of South Norway, and participants provided written informed consent. Participants were required to be right-handed, speak Norwegian fluently and have (corrected to) normal hearing and vision. Clinical sequences (T2-FLAIR) were inspected by a neuroradiologist and deemed free of significant injuries or conditions.

### Non-Human Primates

Evolutionary cortical expansion was calculated from the brains of 4 simian primates: marmoset (*Callithrix jacchus*), capuchin (*Cebus apella*), macaque (*Macaca mulatta*), and human. Details about the calculations have been described in a previous publication (Chaplin et al. 2013). Briefly, surface models of the cerebral cortex of the 4 species were registered by deforming the models to align a set of landmarks, consisting of well-established homologous cortical regions, using the CARET software package (Van Essen et al. 2001). Expansion was calculated as the change in size of each mesh polygon, and was averaged across the marmoset to capuchin, marmoset to macaque, and macaque to human deformations. All tests involving comparisons with evolutionary expansion were restricted to measures extracted from right-hemispheric nodes. For the "State-Dependent Coupling Analyses" (Fig. 2), and the "Developmental Sample Analyses" (Fig. 3), cortical nodes were binned per evolutionary expansion (SFig. 5). We considered the 20% highest-expanding nodes "hotspot" regions, and this definition revealed 3 separate clusters commonly discussed in the literature (Hill et al. 2010; Chaplin et al. 2013).

### Experimental Design

Resting-state fMRI was collected during eyes-closed rest. Participants were instructed to not fall asleep. Given recent reports that eyes-closed resting-state is associated with higher levels of unintentional sleep among participants when compared with eyes-open rest (Tagliazucchi and Laufs 2014), the current sample only included participants that confirmed compliance and reported that they remained awake throughout the scan. During the fMRI-task, participants sequentially viewed 100 line drawings of objects and immediately produced a motor response indicating whether the object was congruent with a spoken action (either "Can you eat it" or "Can you lift it"; SFig. 3). The task is described in detail elsewhere (Sneve et al. 2015).

### MRI Acquisition

Imaging was performed at a Siemens Skyra 3 T MRI unit with a 24-channel head coil. For the fMRI scans (rest and task), 43 slices (transversal, no gap) were measured using T2* BOLD EPI (TR = 2390 ms; TE = 30 ms; flip angle = 90°; voxel size = 3 × 3 × 3 mm; FOV = 224 × 224; interleaved acquisition; GRAPPA = 2). The rsfMRI run produced 150 volumes and lasted ≈6 min. The task data were collected over 2 runs, each consisting of 131 volumes and lasting ≈5.2 min. Three dummy volumes were collected at the start of each fMRI scan to avoid T1 saturation effects in the analyzed data. A standard double-echo gradient-echo field map was acquired for distortion correction of the EPI images. Anatomical T1-weighted MPRAGE images consisting of 176 sagittally oriented slices were obtained using a turbo field

echo pulse sequence (TR = 2300 ms, TE = 2.98 ms, flip angle = 8°, voxel size = 1 × 1 × 1 mm, FOV = 256 × 256 mm).

### MRI Preprocessing

Cortical reconstruction of the T1-weighted scans was performed with Freesurfer 5.3's recon-all routines, and included surface inflation (Fischl et al., 1999a) and registration to a spherical atlas which utilized individual cortical folding patterns to match cortical geometry across subjects (Fischl et al., 1999b). Functional MRI-data were corrected for B0 inhomogeneity, motion and slice timing corrected, and smoothed (5 mm FWHM) in native volume space using FSL (http://fsl.fmrib.ox.ac.uk/fsl/fslwiki). Next, FMRIB's ICA-based Xnoiseifier (FIX; Salimi-Khorshidi et al. 2014) was used to auto-classify noise components and remove them from the fMRI data. Such ICA-based procedure for denoizing fMRI data has been shown to effectively reduce motion-induced variability, outperforming methods based on removing motion spikes in the dataset (Pruim et al., 2015). Importantly, different classifiers were used for rsfMRI and task-fMRI data. Classifiers were trained on scanner-specific datasets in which rsfMRI/task-fMRI data from 16 participants had been manually classified into signal and noise components (fMRI acquisition parameters identical to the current study). Motion confounds (24 parameters) were regressed out of the fMRI data as a part of the FIX routines. Freesurfer-defined individually estimated anatomical masks of cerebral white matter (WM) and cerebrospinal fluid/lateral ventricles (CSF) were resampled to each individual's functional space. Following FIX, average time series were extracted from functional WM- and CSF-voxels and were regressed out of the FIX-cleaned 4D volume. Following recent recommendations (Hallquist et al. 2013) we band-pass filtered the rsfMRI data (0.009–0.08 Hz) after regression of confound variables. Task-fMRI data were detrended and highpass filtered with a 0.01 Hz cutoff.

### Network Analysis of rsfMRI Data

A custom cortical parcellation was created in Freesurfer's average surface space (fsaverage), using a modified N-cut algorithm (Craddock et al. 2012), consisting of 340 (170 per hemisphere) spatially contiguous, approximately equally sized nodes covering the entire cerebral cortex. The parcellation was resampled into each participant's functional volume space using a projection factor of 0.5, i.e., half way into the cortical sheet. For each participant, we extracted mean preprocessed rsfMRI time series from all nodes and calculated a 340 × 340 connectivity matrix consisting of the Pearson's *r* correlations between nodal time series. Next, we Fisher-transformed all participants' connectivity matrices, and averaged across participants to create a "grand average" connectivity matrix on which network analysis was performed. The grand average connectivity matrix was thresholded at 5, 6, 7, 8, 9, 10, 15, and 20% edge densities. For all thresholded weighted graphs, the optimal modular resolution parameter (gamma) promoting stable decomposition results, was calculated using the Versatility approach (Shinn et al. 2017; see SFig1). Next, modular decomposition was performed with the Louvain algorithm (Blondel et al. 2008) as implemented in the Brain Connectivity Toolbox (BCT) (Rubinov and Sporns 2010) and followed by consensus clustering (Sporns and Betzel 2016). Briefly, this involved calculating an agreement matrix from 10 000 independent Louvain partitions, thresholding this empirical agreement matrix by the maximum agreement observed over 10 000 randomly generated null association matrices and running clustering on the thresholded empirical agreement matrix. In the case of singleton partitions, i.e., network modules consisting of one node only – typically consisting of low signal-to-noise regions such as the temporal pole and orbitofrontal cortex – these modules were excluded from the remaining network analyses. Finally, we used the thresholded graphs' optimal community structures to calculate two nodal network measures per graph: *participation coefficient* and *within-module degree*, representing a node's intermodular and intramodular centrality, respectively (Rubinov and Sporns 2010). Two additional measures not requiring information about the underlying community structures were also calculated: *betweenness centrality*, representing the fraction of all shortest paths in the network that contains a given node, and *strength*, the sum of a given node's connectivity weights to every other node (Rubinov and Sporns 2010). Relationships between nodal network measures and estimates of evolutionary expansion were investigated using nonparametric Spearman correlations due to non-normal distributions (assayed using Q–Q plots).

### Community Density Analyses

To investigate high-expanding nodes' anatomical centrality, we used a parcellation of human cortical intrinsic connectivity into 17 canonical networks, estimated from 1000 participants (Yeo et al. 2011). First, we extracted MNI-coordinates for every vertex in the right hemisphere in a downsampled Freesurfer surface representation (fsaverage5; 10 242 vertices). Next, for each vertex, we counted the number of canonical networks present within a radius of 5, 10, 15, 20, 25, and 30 mm (Euclidean distance). For each radius, the number of networks at every vertex was normalized (0–1) by the maximum number of networks found across all vertices (Power et al. 2013). Finally, the normalized community density values were averaged across radii at each vertex, and correlated with evolutionary expansion estimates at the same locations using Spearman correlations (due to non-normal distributions).

### Flexibility Analyses

The functional flexibility of each vertex on the cortical surface of the right hemisphere was estimated from publicly available data (https://surfer.nmr.mgh.harvard.edu/fswiki/BrainmapOntology_Yeo2015). Here, an author-topic hierarchical Bayesian model was used to classify 10 449 experimental contrasts from fMRI experiments found in the BrainMap database (Fox and Lancaster 2002) into 12 underlying cognitive components and corresponding brain activity patterns (Yeo et al. 2015). Flexibility was defined as the number of cognitive components activating a voxel. To account for non-integer values due to projections from volume to surface space we rounded surface flexibility estimates to the nearest integer. A nonparametric Kruskal–Wallis was used to compare central tendencies in evolutionary expansion across flexibility groups due to unequal variances across groups (significant Bartlett's test: $\chi^2(8) = 3549$, $P < 1e{-}10$)

### Task-State Connectivity

Following preprocessing, volumetric task-fMRI data were brought to fsaverage surface space. Here, for each participant, we extracted mean BOLD time series from all nodes in the custom 340-node cortical parcellation. Next, psychophysiological interaction (PPI) terms representing nodal task-related activity

modulations were calculated using the generalized PPI-toolbox for Matlab (McLaren et al. 2012). For each node, this involved: (1) deconvolving the mean BOLD time series into estimates of neural events (Gitelman et al. 2003); (2) setting up a task-regressor representing the combined auditory–visual–motor-event (2 s trial duration, 50 trials per fMRI run) (3) convolving the product of step 1 and 2 with a canonical hemodynamic response function (cHRF). Finally, to establish task-related functional connectivity between nodes, we estimated pairwise interactions between all nodes' PPI-terms (concatenated over runs) using partial correlations. For each pairwise correlation, we controlled for background noise and task stimulation effects using the nodes' mean BOLD time series and the cHRF-convolved task-regressor, respectively. This "correlational PPI" approach has been described in detail elsewhere (Fornito et al. 2012).

## State-Dependent Coupling Analyses

A total of 105 adult participants were represented with matrices of functional connectivity obtained from a resting-state and a task-state. First, the individual connectivity matrices were thresholded to contain only edges surviving FDR-correction ($q < 0.05$). Next, to allow for a comparison of connectivity data from different states, edge-wise connectivity weights were normalized by the average weight in the matrix (Opsahl et al. 2010). After mapping from weights to lengths (inversing the connection-weights matrices), shortest path-lengths were calculated using Dijkstra's algorithm (Dijkstra 1959). A node's closeness centrality was calculated as the inverse of the average of its shortest path-length to every other node. A repeated measures ANOVA with two within-subject factors; "expansion bin" (5 levels) and "state" (2 levels); was performed to compare closeness centrality measures over regions having undergone different amount of expansion in evolution, as a factor of cognitive state.

Note that although estimates of functional connectivity from the two states were derived using different approaches (rest: timeseries correlations; task: correlational PPI), both approaches involve calculating the Pearson's correlation coefficient between the regions' ongoing spontaneous BOLD fluctuations during periods of interest. The state comparisons were also conducted using identical preprocessing and analysis approaches across the states (see "Control Analyses" below).

## Analyses of the Developmental Sample

The developmental sample consisted of the 105 adult participants described in the section State-Dependent Coupling Analyses and 46 participants below 18 years of age (see Human Subjects section). All non-adult participants were preprocessed and analyzed as described for the adult sample. One participant (age 9.3 years) was excluded from the sample due to high levels of motion (mean absolute motion over two task runs > 1.5 mm). A significant positive correlation (Spearman's rho = 0.37, $P < 4e{-}06$) was found in the remaining developmental sample ($N = 150$) between estimated motion during the task-state (first principal component of mean absolute and relative motion over two task runs, explaining 98.1% of the total variance) and global closeness centrality (average closeness centrality over all 170 nodes, corresponding to the graph theoretical measure global efficiency (Rubinov and Sporns 2010)). This positive correlation between subject motion and global closeness centrality indicated that participants with relatively high levels of motion (which is a characteristic of young samples (Satterthwaite et al. 2012)) also tended to show high estimates of closeness centrality. To allow for comparisons of closeness-centrality estimates across age groups, unbiased by motion at the global level, we therefore standardized (z-scored) the estimates on a within-subject basis before comparing relative coupling differences across groups. This effectively removed all correlations with motion also when investigating high-expanding and lower-expanding cortex separately (Spearman's *rho* calculated over 5 expansion bins; lowest expansion to highest expansion: –0.06, 0.14, –0.04, 0.04, –0.01; all P-values > 0.09). Furthermore, we included individual estimates of mean absolute and relative motion as covariates in all statistical tests.

To compare relative coupling across age groups, a repeated measures ANOVA was run with one within-subject factor: "expansion bin" (5 levels), and one between-subject factor: "age group" (2 levels). Mean absolute and relative motion over two task runs were included as covariates. Next, for all 150 participants in the developmental sample, we calculated task-state closeness centrality for each of the 170 nodes in the custom right hemisphere neocortical parcellation and correlated these with evolutionary expansion estimates for the same nodes. We then fitted a nonparametric local smoothing model minimizing the Bayesian information criterion (BIC) to delineate the age trajectory of the relationship between closeness centrality and evolutionary expansion (Fjell et al. 2010). Note that the BIC of the optimal smoothing spline was 8.7 lower than the BIC of a linear fit, indicating that the age trajectories were curvelinear. Confidence intervals of the fit were established using bootstrapping.

Scores on the matrix reasoning and vocabulary subtests of the Wechsler's Abbreviated Scale of Intelligence (WASI; Wechsler 1999) were available from 140 of the participants in the developmental sample (age range 7–38 years). Principal component analysis was run on the raw scores of the two subtests, and the first component, which explained 95.5% of the total variance, was used as a representative measure of general intelligence across participants.

## Weighting by Euclidean Distance

Euclidean distance between nodes in the right hemisphere was calculated as the average distance (in mm) between the locations of their constituent vertices converted to MNI305 space. To calculate the weighted connectivity matrices, the Euclidean distance matrix was normalized to fall between 0 and 1 and multiplied, element-by-element, with the connectivity matrices across states and participants. Such weighting by geometric distance has been shown to increase sensitivity in detecting graded network differences (Liu et al., 2014), and was applied in all analyses performed on the single-subject level involving comparisons between states or individuals (i.e., the state-dependent coupling analyses (Fig. 2), and the analyses of the developmental sample (Fig. 3)). As the network analyses of the rsfMRI data (Fig. 1*b*) were performed on the grand-average graph and required community detection steps (for which distance weighting would produce networks not comparable to those typically shown in the literature), we conducted these analyses on unweighted data. However, for comparison, the correlations between nodal evolutionary expansion and graph metrics following weighting by Euclidean distance are shown in SFigure 2.

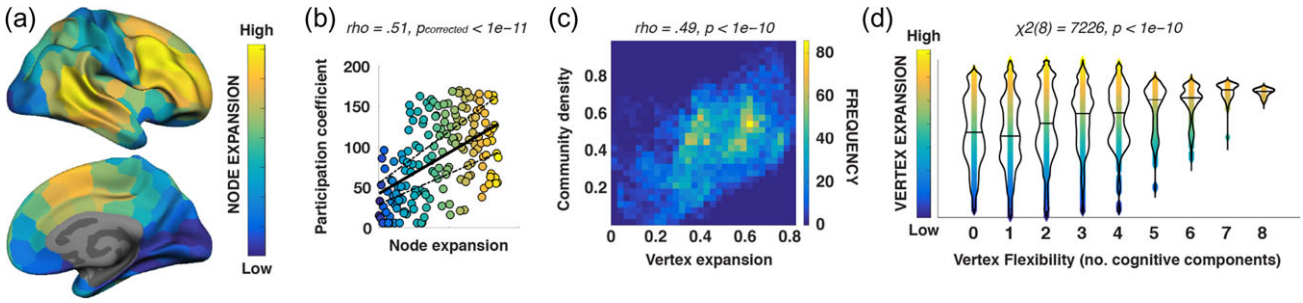


**Figure 1.** High-expanding cortex has broad functional connections and is flexibly engaged across different cognitive tasks. (*a*) Estimates of evolutionary expansion for 170 similarly sized nodes covering the right hemisphere. (*b*) Spearman correlation between node expansion and node participation coefficient. The presented values are averaged across thresholds and ranked – plotted linear relationship thus represent the Spearman correlation. Observed (non-ranked) participation coefficient values scaled between 0 and 0.71. Traditional hub-measures not incorporating integrative aspects of nodal communication (within-module degree, node strength), did not show any relationships with node expansion (SFig. 1*c*). (*c*) Density plot showing the Spearman correlation between vertices' normalized community and estimated evolutionary expansion. (*d*) Violin plots showing the relationship between cortical expansion and cognitive flexibility at the vertex level. Median expansion is shown as horizontal lines. A Kruskal–Wallis test confirmed that expansion differed across flexibility groups. Post-hoc pairwise comparisons demonstrated that cortical locations involved in 5 or more cognitive components were more expanded than locations involved in four or less components ($P < 1.25e{-}07$). All reported *P*-values are corrected for multiple tests.

### Control Analyses

Three series of additional control analyses were carried out to test whether the observed effects were consistent across different analytic choices. First, we performed the state-dependent coupling analyses on edge weights directly, i.e., avoiding the step of mapping weights to lengths. Rather than estimating *closeness centrality*, here we conceptualized a node's centrality as its average correlation to all other nodes in the parcellation (see SFig. 6*B*). SFigure 7*B* depicts the same analyses performed on data not weighted by Euclidean distance between nodes.

In a second set of control analyses, we estimated task-state functional connectivity using time-series correlations rather than correlational PPI. Here, data from both task-state runs were preprocessed and analyzed in a similar fashion as the resting-state data. This resulted in two functional connectivity graphs (one per run) per participant, which were averaged before being compared with the resting-state data (see SFig. 6*C* and the associated caption). SFigure 7*C* depicts the same analyses performed on data not weighted by Euclidean distance between nodes.

The third set of control analyses involved the regression of motion estimates (mean absolute and relative motion) from the functional connectivity graphs in the developmental sample before comparing relative coupling of high-expanding nodes across age groups. Regression was performed across subjects at the edge-level (i.e., all region-to-region connectivity estimates were corrected). The relevant results following motion regression are shown in SFigure 8.

Across all presented analyses, all tests were two-tailed.

## Results

### High-Expanding Cortex has Broad Functional Connections and is Engaged Flexibly Across Different Cognitive Tasks

First, we tested whether high-expanding nodes communicate more broadly across human functional brain networks than low-expanding nodes. Investigations in the macaque monkey have demonstrated strong positive relationships between dendritic complexity at the microscale neuronal level, and broadness of cortico-cortical neuronal connectivity profiles at the macroscale network level (Scholtens et al. 2014). Therefore, we tested whether high-expanding nodes are characterized by high *participation coefficients*, a graph theoretical measure that quantifies the degree to which a node participates in many of the brain's subnetworks (Guimerà and Nunes Amaral 2005). Functional connectivity between nodes covering the entire cerebral cortex was calculated from resting-state functional MRI (rsfMRI) data from 221 healthy young adults. We estimated optimal community structures, i.e., the brain's subnetworks, through modular decomposition of the group-averaged connectivity graph thresholded at different edge densities (SFig. 1*a*&*b*). Next, for each threshold, we calculated every node's participation coefficient – a high value indicating that it connects functionally outside its own community. Finally, we extracted average nodal expansion between three non-human simian primates and humans from estimates of evolutionary cortical scaling (Chaplin et al. 2013) (Fig. 1*a*). A positive relationship was found between nodal participation coefficient values and estimates of evolutionary expansion at all edge densities (Fig. 1*b* and SFig. 1*c*), suggesting that high-expanding regions function as integrative connector nodes in the information flow between more specialized modules in human cortex (Power et al. 2013). In line with this observation, nodal *betweenness centrality* also correlated positively with expansion (SFig. 1*c*), demonstrating that high-expansion regions often participate in the shortest, most efficient, functional path between any two other nodes in the brain network (Rubinov and Sporns 2010).

Next, we tested whether the topologically broad and central functional connectivity profiles of high-expanding nodes – as indicated by high participation coefficient and betweenness centrality, respectively – were reflected in their anatomical centrality relative to the canonical functional networks of the human brain (Yeo et al. 2011). The measure *community density* represents the number of different networks present within a given radius from a cortical location (Power et al. 2013). We observed a positive relationship between local surface expansion and community density, indicating that high-expanding parts of the cortex have access to multiple networks present in their immediate vicinity (Fig. 1*c*). This closeness, both at the anatomical and the network topology-level, between high-expanding parts of the cortex and the brain's different networks, makes high-expanding cortex ideally situated to engage in a variety of cognitive processes. To test this hypothesis, we took advantage of recent work on the BrainMap database, in

which data from ≈10.000 fMRI-experiments have been merged to establish brain activity patterns common to specific types of tasks (Yeo et al. 2015). We grouped cortical surface locations based on the number of task-types ("cognitive components") they were associated with, and then compared expansion across these levels of cognitive flexibility. In line with our hypothesis, highly flexible nodes were found predominantly in high-expanding cortex (Fig. 1*d*).

## High-Expanding Cortex Communicates Preferentially With Regions Engaged by the Current Cognitive Demands

The above findings suggest that a key role of high-expanding cortical regions may be integration of different cognitive processes. To test this proposal directly, we estimated the *closeness centrality* of cortical nodes in 105 participants scanned using fMRI during two states: unconstrained rest, and a task-state requiring audio-visuo-motor processing (SFig. 3). Closeness centrality represents the average shortest path-length from one node to all other nodes in a network, and thus indicates how tight the functional coupling of a node is to the rest of the network (Rubinov and Sporns 2010). High-expanding regions showed higher closeness centrality during the task-state than during rest and were also more tightly coupled to the rest of the network than lower-expanding nodes (Fig. 2*a*). Critically, this was also true when accounting for physical (Euclidean) distance between nodes, demonstrating that the tight functional coupling of high-expanding nodes to the rest of the network during multimodal integration is independent of their physical locations on the cortical surface (Liu et al. 2014) (SFig. 4). The higher closeness centrality during the task-state was distributed across all high-expanding regions (Fig. 2*b*), suggesting that stronger functional coupling during effortful task-operations is a general property of high-expanding cortex and not driven by a subset of cortical regions.

To test the key proposal that evolutionary high-expanding cortex play a central role in *supramodal* cognition – and thus interact flexibly with different parts of cortex depending on particular cognitive demands – we calculated functional coupling change (resting-state to task-state) between high-expanding regions and all cortical nodes. During the multimodal task-state, their coupling increased (i.e., path length decreased) most prominently with posterior visual perceptual regions, auditory cortex and motor cortex (Fig. 2*c*). In support of the hypothesis that high-expanding cortex connects with regions engaged during a given cognitive state, these regions also showed upregulated functional coupling between themselves during the task state when compared with rest (Fig. 2*d*). Critically, medial temporal cortex and ventromedial prefrontal cortex, regions found to be involved in memory consolidation processes during offline rest (van Kesteren et al. 2010; Euston et al. 2012), showed the opposite pattern: stronger functional coupling with high-expanding cortex during rest than during the task state (Fig. 2*c*). Moreover, and in direct accordance with the proposal that evolutionary high-expanding cortex interact

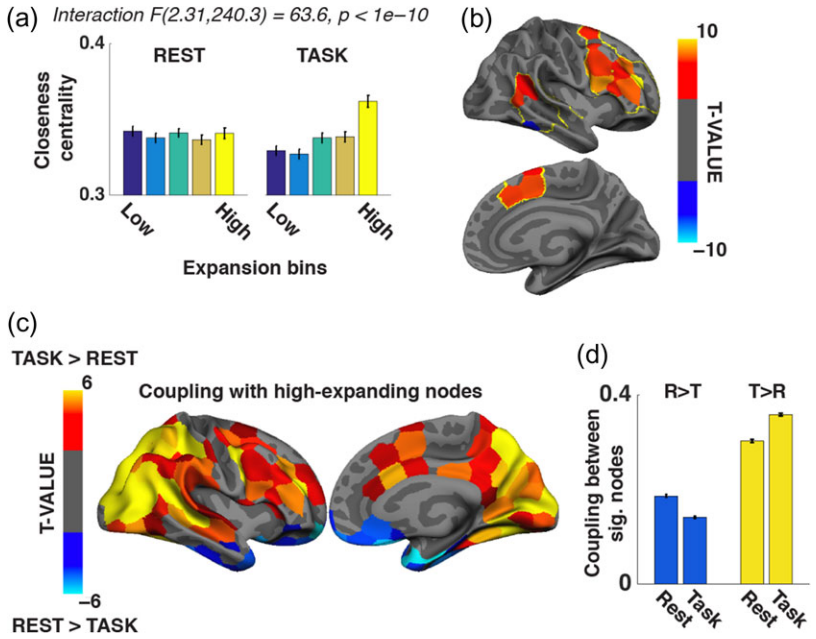


**Figure 2.** High-expanding cortex communicates differently depending on the current cognitive demands, and preferentially with regions engaged by those demands. (*a*) Average closeness centrality for 5 expansion bins during resting- and task-state (dark blue: 20% least expanding nodes, yellow: 20% most-expanding nodes; intermediate colors: intermediate expansion levels). Following a significant "expansion bin X state" repeated measures ANOVA (Greenhouse-Geisser corrected following a significant Mauchly's test of sphericity: $\chi^2$ (9) = 129, $P$ < 1e–10), paired-samples *t*-tests showed significant increase in closeness centrality in task- compared with resting-state for the highest-expanding nodes only: $t(104) = 4.27$, $p_{FDR} < 5.0e–04$. (*b*) Nodes within expansion hotspot regions (indicated by yellow lines) showing significant (paired-samples *t*-tests, $p_{FDR} < 0.05$) changes in closeness centrality from rest to task. (*c*) Nodes showing significant change (paired-samples *t*-tests, $p_{FDR} < 0.05$) in functional coupling with expansion hotspots from rest to task across participants. (*d*) Mean functional coupling between nodes showing negative (blue)/positive effect (yellow) in panel *c*. Nodes falling within the expansion hotspot regions were excluded when calculating the mean. Nodes more strongly coupled with high-expanding regions during rest (R > T) showed higher coupling with each other during rest than during task: paired-samples *t*-test, $t(104) = -10.56$, $p_{FDR} < 3.7e–18$. The opposite effect was observed between nodes more strongly coupled with high-expanding regions during the task-state (T > R): paired-samples *t*-test, $t(104) = 13.25$, $p_{FDR} < 4.4e–24$. The presented data have been weighted by Euclidean distance between nodes. Unweighted data show similar effects (SFig. 6A). All reported *P*-values are corrected for multiple tests. Error bars represent SEM.

flexibly with regions engaged in a given cognitive state, functional coupling between these regions was upregulated during rest when compared with the task-state (Fig. 2*d*).

## Human Development of Neocortical Functional Coupling Patterns Follows Evolutionary Expansion Trajectories

Recent investigations of neocortical morphometry have found similarities between cortical expansion in human development and primate evolution (Fjell et al. 2015). Evolutionary high-expanding cortex, in particular, shows protracted development, and undergoes larger increases in surface area between infancy and adulthood than lower-expanding regions (Hill et al. 2010; Amlien et al. 2016). Notably, this pattern of surface change during development is more pronounced in high-intelligence samples (Schnack et al. 2015), lending support to the idea that similar developmental and evolutionary trajectories of neocortical change – albeit at very different scales – may promote the same phenotypic characteristics of higher intellectual abilities and supramodal cognition.

To test whether such correspondence exists between neocortical evolution and functional supramodal cognition characteristics in human cortical development, we collected task-state fMRI data from 46 children and adolescents (6–17 years of age, one excluded due to excessive motion), and compared closeness centrality estimates from regions differing in evolutionary expansion. As found in the adult sample, high-expanding regions' closeness centrality was higher during the multimodal task state also in the children when compared with lower-expanding parts of cortex (Fig. 3*a*). Additionally, an interaction was observed between age group and regional expansion, indicating that the relative coupling differences between higher- and lower-expanding regions change during development. Specifically, high-expanding cortex' closeness centrality relative to the typical (average) centrality across all nodes, i.e., its relative coupling, was found to be less developed in the young sample when compared with the adults (Fig. 3*a*). Importantly, less-expanding regions did not show significant differences in coupling between the two age groups. This observation fits well with recent reports of protracted surface area development of evolutionary high-expanding regions, reaching maximum expansion in adolescence (Amlien et al. 2016; Walhovd et al. 2016), and suggests that their roles as multimodal integrating hubs follow related developmental trajectories.

Finally, if evolutionary factors have shaped ontogenetic cortical development, we would expect the mature human brain to reflect the changes that have occurred in primate evolution to a higher degree than the immature brain (e.g., Rakic 2009). For all 150 participants in the adult and development sample, we calculated task-state closeness centrality for each of the 170 nodes in the custom neocortical parcellation and correlated these with evolutionary expansion estimates for the same nodes. Next, we fitted a nonparametric local smoothing model (Fjell et al. 2010) to delineate the age trajectory of the relationship between closeness centrality and evolutionary expansion. The relationship was found to be not significant until approximately 18 years of age, at which point the fit revealed positive correlations between neocortical functional coupling pattern and expansion (Fig. 3*b*). Interestingly, and in line with previous morphometric reports (Fjell et al. 2015; Schnack et al. 2015), participants showing higher similarity between their nodal centrality maps and the evolutionary expansion map were characterized by higher scores on measures of general intelligence (Fig. 3*c*). This suggests that evolutionary concepts resonating in the functional coupling of the human neocortex are relevant for the characteristic human phenotype of higher intellectual function.

## Control Analyses

The control analyses (presented in SFig. 6–8) supported the main findings reported above. One discrepancy was however observed: when analyzing task data following the resting-state analysis approach (SFig. 6C+7C), we did not observe stronger coupling between high-expanding cortex and medial temporal/ventromedial prefrontal cortex during rest when compared with the multimodal task-state. We suspect this may be due to the task time series also containing long periods of rest during the inter-trial intervals. While these inter-trial rest periods

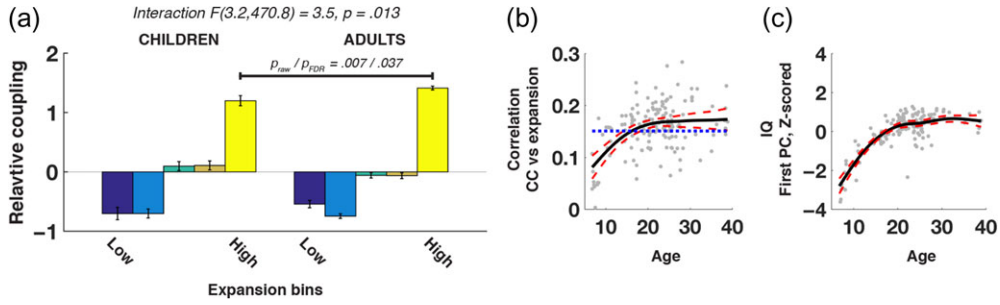


**Figure 3.** Human development of neocortical multimodal coupling patterns follows evolutionary expansion trajectories. (*a*) High-expanding cortex showed stronger relative coupling than lower-expanding regions in both age groups (children: $t(44) > 8.09$, $p_{FDR} < 3.0e{-}10$; adults: $t(104) > 23.73$, $p_{FDR} < 1.0e{-}10$). Following the significant "age group × expansion bin" interaction (Greenhouse-Geisser corrected following a significant Mauchly's test of sphericity: $\chi^2(9) = 63.6$, $P < 3e{-}10$), post hoc tests showed lower relative coupling of high-expanding nodes in the development sample compared with the adults ($Z = -2.68$, $p_{FDR} < 0.037$; Wilcoxon rank sum due to unequal variances across groups: Bartlett's test: $\chi^2(1) = 20.8$, $P < 6e{-}06$). Lower-expanding nodes did not show significant differences in relative coupling between age groups ($p_{FDR} > 0.093$). Error bars represent SEM. (*b*) Individual correlation between nodal closeness centrality and evolutionary expansion plotted as a function of age. The black line represents the best fitting smoothing spline. Red lines represent the bootstrapped 95% confidence interval of the fit. Blue dotted line shows the correlation coefficient at which a correlation with 169 degrees of freedom is significant at $P < 0.05$ (abs(rho) > 0.151). (*c*) First principal component calculated from raw scores on two WASI subtests plotted as a function of age. Spearman correlations revealed significant relationships between this measure of general intelligence and individual differences in closeness centrality-vs-expansion correlation (i.e., correlating data points in Figure 3*b* and *c*: Spearman's rho = 0.34, $P < 4.9e{-}5$). Importantly, this relationship remained when controlling for nonlinear influences of age using partial Spearman correlations (rho = 0.184, $P = 0.030$), and when including motion estimates (in addition to age) as control variables (rho = 0.177, $P = 0.039$)

were effectively excluded in the main analyses using the correlational PPI approach, they remained present in the control analyses since functional connectivity here was defined as correlations between BOLD time-series covering the full task runs, i.e., without discriminating between state changes within the runs.

## Discussion

Our findings point to a central role of evolutionary high-expanding cortex in integrative operations during a variety of cognitive states. The functional signature of such supramodal cognition matures throughout childhood, suggesting that the high-expanding regions develop their characteristic of broad functional connections to many of the brain's networks in tandem with the emergence and refinement of central human cognitive skills. Their postulated overarching function in facilitating supramodal and flexible cognition is supported by the reported links between general intelligence and surface area of high-expanding regions (Fjell et al. 2015; Schnack et al. 2015). Moreover, the functional connectivity "fingerprints" of high-expanding cortex have been shown to be highly variable from participant to participant, and these characteristic overlaps well with the degree to which a brain region can be used to predict performance during different types of cognition (Mueller et al. 2013). The underlying cellular machinery appears optimized to support such supramodal processes: neuromorphological investigations of primate cortex have found more elaborate dendritic layouts in high-expanding compared with low-expanding regions (Elston et al. 1999), and these structural properties are more pronounced in humans than in non-human primates (Bianchi et al. 2013; Geschwind and Rakic 2013; Donahue et al. 2018).

In the current study, we interpret cortical regions demonstrating the capacity to integrate information from across the brain in a flexible manner as to take part in supramodal cognition. The claim that certain parts of the cortex, and in particular prefrontal regions, play such flexible integrative roles is hardly new (e.g., Goldman-Rakic 1988), however we believe there is novelty in linking these broad functions to evolutionary morphological changes and their candidate behavioral phenotypes. Our results suggest that, when analyzed as a unit, high-expanding cortex shows both integrative and supramodal characteristics. However, the regions constituting the expansion "hotspots" are spread in a partly discontinuous manner across large portions of the cortex and may show different characteristics and specializations when investigated in a more fine-grained fashion (Chaplin et al. 2013). A fascinating venue for further research could be to collect data on unimodal in addition to multimodal tasks in an attempt to disentangle modality-specific from integrative functions. Specifically, regions showing increased task-related recruitment and/or functional coupling during multimodal states when compared with unimodal states could be said to be integrative, while regions demonstrating differential coupling patterns over varying task-requirements would support supramodal flexibility. The current results suggest that one would find regions fulfilling both criteria primarily within evolutionary high-expanding cortex.

### Methodological Considerations and Limitations

While measures of functional connectivity may be reflective of underlying anatomical connectivity (Vincent et al. 2007; Honey et al. 2009; Hermundstad et al. 2013), they are nevertheless estimated from covariations in signal time-series and can thus be affected by mechanisms other that direct interactions between neuronal populations. In the current study, we do not base any conclusions on observations from single edges (i.e., simple bivariate correlations between two regions), but rely on graph theoretical nodal summary measures – such as closeness centrality – and regions' relative roles in the brain network along these measures. Moreover, due to the within-subject nature of our coupling analyses, we base our conclusions about high-expanding cortex and supramodality on the observed consistent *modulations* in functional coupling across states, not the presence/absence of specific connections. It should be stressed that path-based graph metrics, when estimated from functional connectivity networks, are statistical constructs that do not necessarily reflect information flow along anatomical connections in the brain (Rubinov and Sporns 2010; Smith et al., 2013; Fornito et al., 2016). The successful use of functional path-length measures as predictors of cognition (e.g., Bassett et al., 2009; van den Heuvel et al., 2009; Kinnison et al., 2012), and observations that such metrics are under genetic control (Fornito et al., 2011; van den Heuvel et al., 2013; Sinclair et al., 2015), suggests that they reflect biologically meaningful processes and network characteristics. At present, however, shortest path-length measures derived from correlation-based functional networks should not be considered as direct anatomical links. In the current study, we observe similar effects when calculating coupling based on raw correlation weights rather than path-length measures (SFig. 6*B* and 7*B*). While this suggests that the observed strong centrality of evolutionary high-expanding regions during multimodal cognitive operations is not an artifact of converting weights to lengths, edge-correlation weights have limited interpretability in terms of anatomical pathways as they can reflect both direct couplings between nodes and interactions via intermediate regions (Fornito et al., 2016).

Some uncertainty is also associated with the reported relationship between nodal participation coefficient and evolutionary expansion (i.e., Fig. 1*b*) as they were derived from group averaged graphs of functional connectivity and network parcellations of these. Interestingly, recent work on individual-specific network parcellations (e.g., Gordon et al., 2017; Kong et al., 2018) have suggested that the size, location, and spatial arrangement of cortical networks differ (to some degree) between participants. A common observation in these studies seems to be higher intersubject variability in the spatial layout of association networks when compared with sensory-/motor-networks (Laumann et al., 2015; Wang et al., 2015; Kong et al., 2018), in line with the idea that the development of areas in these networks is less constrained by molecular specification steps in early development (Rosa and Tweedale 2005). In principle, the high participation coefficients observed in high-expanding association cortex when calculated from the group averaged graphs – indicating strong functional coupling across networks – could thus in part be reflective of heterogeneity in the network profiles at the individual level. We are not, however, aware that there is any consensus about how to navigate between individual-specific and group-level based network parcellations and interpret the observed topographical discrepancies. As reliable estimates of the participation coefficient at the individual level are hard to establish even with extensive periods of resting-state data per participant (Gordon et al., 2017), we have here tried to take an alternative approach by investigating high-expanding cortex' postulated integrative role using a variety of measures and approaches. Thus, while keeping the

important limitations discussed above in mind, we believe our general claims are supported and strengthened by the observed consistencies across modalities (Community Density Analyses) and with independent datasets (Flexibility Analyses), as well as by the replication of selective increase in high-expanding cortex' functional coupling during multimodal requirements across two independent groups of participants (Developmental Sample Analyses).

The observed correlations between our measures of functional coupling and registered head motion in the developmental sample were mitigated through standardization at the individual data level, and by including individual motion estimates as covariates at the statistical level. Per-individual standardization of closeness centrality coupling measures effectively removed potential global effects of motion (i.e., affecting all regions) on the centrality measures. Importantly, the standardization step also removed all observed significant correlations between motion and centrality measures when investigating regions characterized by different amounts of evolutionary expansion – "expansion bins" – separately. In other words, after removing potential global effects of head motion from the data, no correlation was found between individual differences in functional coupling of high-expanding cortex and motion (nor for any other expansion bin). Nevertheless, we included an additional control analysis in which motion estimates across subjects were aggressively regressed in an edge-wise fashion from the participant graphs in the developmental sample. While the effects reported in Figure 3*a* were only marginally influenced by this additional data cleaning step (see SFig. 8), it should be noted that the correction likely affected shared variance between motion and age-normalized participant IQ (Spearman's *rho* = –0.24, P = 0.005), and participant age (Spearman's *rho* = –0.39; P = 7.3e–07), that is, variables found to be associated with the function and development of high-expanding cortex (Hill et al., 2010; Schnack et al. 2015).

The present study is based on interpretation of functional data obtained in humans, correlated with estimates of the differential expansion of parts of the cerebral cortex in primate evolution. To date, these estimates have been derived from careful histological reconstruction of single individual brains from different species, followed by computational registration of 3-dimensional models (Chaplin et al. 2013). The reliance of these estimates on individual brains, rather than population averages, represents a possible limitation of the precision of the present analyses. It should be noted, however, that the differences in expansion that underlie our conclusions are very substantial, relative to the likely degree of individual variation, or errors derived from incorrect assignment of cytoarchitectural boundaries. For example, the differential expansion between the most notable expansion "hotspots" (temporoparietal junction, ventrolateral prefrontal cortex, and dorsal anterior cingulate cortex) and other regions, such as the primary visual cortex and parahippocampal gyrus, is as high as 16-fold between macaque and human (Hill et al. 2010), which is well beyond the variation observed in the volumes of cytoarchitectural areas between individuals of a single primate species (cf. Majka et al. 2016; Woodward et al. 2018). Moreover, although quantitative details of the expansion of different cortical nodes vary slightly depending on which species are used for comparison, the locations of the expansion "hotspots" are remarkably stable (Chaplin et al. 2013). Finally, although some controversy remains about the relative expansion of some regions of the cerebral cortex in primate evolution (e.g., frontal lobe; Barton and Venditti 2013; Sherwood and Smaers 2013), it must be noted that the estimates used in the present study are based on quantitative analyses of species to species registration that took into consideration cytoarchitectural boundaries of areas that are well-defined, rather than gross morphological features of the brain; recent studies that also used cytoarchitecture to guide registration have confirmed that differential expansion exists (Mansouri et al. 2017; Donahue et al. 2018).

## Conclusion

The present results add to existing knowledge by showing how evolutionary high-expanding regions change in their role as communication hubs in different cognitive states, and that this power gradually emerges during childhood and adolescence development.

## Supplementary Material

Supplementary material is available at *Cerebral Cortex* online.

## Funding

This work was supported by the Norwegian Research Council (Grants to A.M.F and K.B.W.), the European Research Council Starting Grant and Consolidator Grant scheme under grant agreements 283634 and 725025 (to A.M.F.) and 313440 (to K.B.W.), as well as the Department of Psychology, University of Oslo (to K.B.W., A.M.F.). The comparative data were obtained with funding of the Australian Research Council.

## Notes

We would like to thank Ed Bullmore (University of Cambridge) for helpful comments on an earlier draft of the manuscript, and Didac Vidal Piñeiro (University of Oslo) for help with analyses. *Conflict of Interest*: The authors declare no competing interests.

## References

Amlien IK, Fjell AM, Tamnes CK, Grydeland H, Krogsrud SK, Chaplin TA, Rosa MGP, Walhovd KB. 2016. Organizing principles of human cortical development - thickness and area from 4 to 30 years: insights from comparative primate neuroanatomy. Cereb Cortex. 26:257–267.

Barton RA, Venditti C. 2013. Human frontal lobes are not relatively large. Proc Natl Acad Sci. 110:9001–9006.

Bassett DS, Bullmore ET, Meyer-Lindenberg A, Apud JA, Weinberger DR, Coppola R. 2009. Cognitive fitness of cost-efficient brain functional networks. Proc Natl Acad Sci. 106: 11747–11752.

Bianchi S, Stimpson CD, Bauernfeind AL, Schapiro SJ, Baze WB, McArthur MJ, Bronson E, Hopkins WD, Semendeferi K, Jacobs B, et al. 2013. Dendritic morphology of pyramidal neurons in the chimpanzee neocortex: regional specializations and comparison to humans. Cereb Cortex. 23: 2429–2436.

Blondel VD, Guillaume J-L, Lambiotte R, Lefebvre E. 2008. Fast unfolding of communities in large networks. J Stat Mech Theory Exp. 10008:6.

Buckner RL, Krienen FM. 2013. The evolution of distributed association networks in the human brain. Trends Cogn Sci. 17:648–665.

Chaplin TA, Yu H-H, Soares JGM, Gattass R, Rosa MGP. 2013. A conserved pattern of differential expansion of cortical areas in simian primates. J Neurosci. 33:15120–15125.

Craddock RC, James GA, Holtzheimer PE, Hu XP, Mayberg HS. 2012. A whole brain fMRI atlas generated via spatially constrained spectral clustering. Hum Brain Mapp. 33:1914–1928.

Dijkstra EW. 1959. A note on two problems in connexion with graphs. Numer Math. 1:269–271.

Donahue CJ, Glasser MF, Preuss TM, Rilling JK, Van Essen DC. 2018. Quantitative assessment of prefrontal cortex in humans relative to nonhuman primates. Proc Natl Acad Sci USA. 115:E5183–E5192. 201721653.

Elston GN, Tweedale R, Rosa MGP. 1999. Cortical integration in the visual system of the macaque monkey: large-scale morphological differences in the pyramidal neurons in the occipital, parietal and temporal lobes. Proc R Soc B Biol Sci. 266:1367–1374.

Euston DR, Gruber AJ, McNaughton BL. 2012. The role of medial prefrontal cortex in memory and decision making. Neuron. 76:1057–1070.

Fischl B, Sereno MI, Dale AM. 1999a. Cortical surface-based analysis: II: Inflation, flattening, and a surface-based coordinate system. Neuroimage 9:195–207.

Fischl B, Sereno MI, Tootell RBH, Dale AM. 1999b. High-resolution intersubject averaging and a coordinate system for the cortical surface. Hum Brain Mapp 8:272–284.

Finlay BL, Darlington RB. 1995. Linked regularities in the development and evolution of mammalian brains. Science. 268: 1578–1584.

Fjell AM, Walhovd KB, Westlye LT, Østby Y, Tamnes CK, Jernigan TL, Gamst A, Dale AM. 2010. When does brain aging accelerate? Dangers of quadratic fits in cross-sectional studies. Neuroimage. 50:1376–1383.

Fjell AM, Westlye LT, Amlien I, Tamnes CK, Grydeland H, Engvig A, Espeseth T, Reinvang I, Lundervold AJ, Lundervold A, et al. 2015. High-expanding cortical regions in human development and evolution are related to higher intellectual abilities. Cereb Cortex. 25:26–34.

Fonseca-Azevedo K, Herculano-Houzel S. 2012. Metabolic constraint imposes tradeoff between body size and number of brain neurons in human evolution. Proc Natl Acad Sci USA. 109:18571–18576.

Fornito A, Harrison BJ, Zalesky A, Simons JS. 2012. Competitive and cooperative dynamics of large-scale brain functional networks supporting recollection. Proc Natl Acad Sci USA. 109:12788–12793.

Fornito A, Zalesky A, Bullmore ET (editors). 2016. Chapter 7 - Paths, diffusion, and navigation. In: Fundamentals of Brain Network Analysis. San Diego: Academic Press. p. 207–255.

Fornito A, Zalesky A, Bassett DS, Meunier D, Ellison-Wright I, Yucel M, Wood SJ, Shaw K, O'Connor J, Nertney D, et al. 2011. Genetic influences on cost-efficient organization of human cortical functional networks. J Neurosci. 31:3261–3270.

Fox PT, Lancaster JL. 2002. Opinion: mapping context and content: the brainmap model. Nat Rev Neurosci. 3:319–321.

Geschwind DH, Rakic P. 2013. Cortical evolution: judge the brain by its cover. Neuron. 80:633–647.

Gitelman DR, Penny WD, Ashburner J, Friston KJ. 2003. Modeling regional and psychophysiologic interactions in fMRI: the importance of hemodynamic deconvolution. Neuroimage. 19:200–207.

Goldman-Rakic PS. 1988. Topography of cognition: parallel distributed networks in primate association cortex. Annu Rev Neurosci. 11:137–156.

Gordon EM, Laumann TO, Gilmore AW, Newbold DJ, Greene DJ, Berg JJ, Ortega M, Hoyt-Drazen C, Gratton C, Sun H, et al. 2017. Precision functional mapping of individual human brains. Neuron. 95:791–807.e7.

Guimerà R, Nunes Amaral LA. 2005. Functional cartography of complex metabolic networks. Nature. 433:895–900.

Hallquist MN, Hwang K, Luna B. 2013. The nuisance of nuisance regression: spectral misspecification in a common approach to resting-state fMRI preprocessing reintroduces noise and obscures functional connectivity. Neuroimage. 82C:208–225.

Herculano-Houzel S. 2011. Scaling of brain metabolism with a fixed energy budget per neuron: implications for neuronal activity, plasticity and evolution. PLoS One. 6:e17514.

Herculano-Houzel S. 2012. The remarkable, yet not extraordinary, human brain as a scaled-up primate brain and its associated cost. Proc Natl Acad Sci. 109:10661–10668.

Hermundstad AM, Bassett DS, Brown KS, Aminoff EM, Clewett D, Freeman S, Frithsen A, Johnson A, Tipper CM, Miller MB, et al. 2013. Structural foundations of resting-state and task-based functional connectivity in the human brain. Proc Natl Acad Sci USA. 110:6169–6174.

Hill J, Inder T, Neil J, Dierker D, Harwell J, Van Essen D. 2010. Similar patterns of cortical expansion during human development and evolution. Proc Natl Acad Sci USA. 107:13135–13140.

Honey CJ, Sporns O, Cammoun L, Gigandet X, Thiran JP, Meuli R, Hagmann P. 2009. Predicting human resting-state functional connectivity from structural connectivity. Proc Natl Acad Sci USA. 106:2035–2040.

Kinnison J, Padmala S, Choi J-M, Pessoa L. 2012. Network analysis reveals increased integration during emotional and motivational processing. J Neurosci. 32:8361–8372.

Kong R, Li J, Orban C, Sabuncu MR, Liu H, Schaefer A, Sun N, Zuo X-N, Holmes AJ, Eickhoff SB, et al. 2018. Spatial topography of individual-specific cortical networks predicts human cognition, personality, and emotion. Cereb Cortex. doi: 10.1093/cercor/bhy123.

Krienen FM, Yeo BTT, Buckner RL. 2014. Reconfigurable task-dependent functional coupling modes cluster around a core functional architecture. Philos Trans R Soc Lond B Biol Sci. 369: 20130526. doi:10.1098/rstb.2013.0526.

Laumann TO, Gordon EM, Adeyemo B, Snyder AZ, Joo SJ, Chen MY, Gilmore AW, McDermott KB, Nelson SM, Dosenbach NUF, et al. 2015. Functional system and areal organization of a highly sampled individual human brain. Neuron. 87:657–670.

Liu Y, Yu C, Zhang X, Liu J, Duan Y, Alexander-Bloch AF, Liu B, Jiang T, Bullmore E. 2014. Impaired long distance functional connectivity and weighted network architecture in alzheimer's disease. Cereb Cortex. 24:1422–1435.

Majka P, Chaplin TA, Yu HH, Tolpygo A, Mitra PP, Wójcik DK, Rosa MGP. 2016. Towards a comprehensive atlas of cortical connections in a primate brain: mapping tracer injection studies of the common marmoset into a reference digital template. J Comp Neurol. 524:2161–2181.

Mansouri FA, Koechlin E, Rosa MGP, Buckley MJ. 2017. Managing competing goals – a key role for the frontopolar cortex. Nat Rev Neurosci. 18:645–657.

McLaren DG, Ries ML, Xu G, Johnson SC. 2012. A generalized form of context-dependent psychophysiological interactions (gPPI): a comparison to standard approaches. Neuroimage. 61:1277–1286.

Mueller S, Wang D, Fox MD, Yeo BTT, Sepulcre J, Sabuncu MR, Shafee R, Lu J, Liu H. 2013. Individual variability in functional connectivity architecture of the human brain. Neuron. 77:586–595.

Opsahl T, Agneessens F, Skvoretz J. 2010. Node centrality in weighted networks: generalizing degree and shortest paths. Soc Networks. 32:245–251.

Power JD, Schlaggar BL, Lessov-Schlaggar CN, Petersen SE. 2013. Evidence for hubs in human functional brain networks. Neuron. 79:798–813.

Pruim RHR, Mennes M, Buitelaar JK, Beckmann CF. 2015. Evaluation of ICA-AROMA and alternative strategies for motion artifact removal in resting-state fMRI. Neuroimage. 112:278–287.

Rakic P. 2009. Evolution of the neocortex: a perspective from developmental biology. Nat Rev Neurosci. 10:724–735.

Rilling JK. 2014. Comparative primate neuroimaging: insights into human brain evolution. Trends Cogn Sci. 18:46–55.

Ringo JL. 1991. Neuronal interconnection as a function of brain size. Brain Behav Evol. 38:1–6.

Rosa MGP, Tweedale R. 2005. Brain maps, great and small: lessons from comparative studies of primate visual cortical organization. Philos Trans R Soc Lond B Biol Sci. 360:665–691.

Rubinov M, Sporns O. 2010. Complex network measures of brain connectivity: uses and interpretations. Neuroimage. 52:1059–1069.

Salimi-Khorshidi G, Douaud G, Beckmann CF, Glasser MF, Griffanti L, Smith SM. 2014. Automatic denoising of functional MRI data: combining independent component analysis and hierarchical fusion of classifiers. Neuroimage. 90: 449–468.

Satterthwaite TD, Wolf DH, Loughead J, Ruparel K, Elliott MA, Hakonarson H, Gur RC, Gur RE. 2012. Impact of in-scanner head motion on multiple measures of functional connectivity: relevance for studies of neurodevelopment in youth. Neuroimage. 60:623–632.

Schnack HG, van Haren NEM, Brouwer RM, Evans A, Durston S, Boomsma DI, Kahn RS, Hulshoff Pol HE. 2015. Changes in thickness and surface area of the human cortex and their relationship with intelligence. Cereb Cortex. 25: 1608–1617.

Scholtens LH, Schmidt R, de Reus MA, van den Heuvel MP. 2014. Linking macroscale graph analytical organization to microscale neuroarchitectonics in the macaque connectome. J Neurosci. 34:12192–12205.

Sherwood CC, Smaers JB. 2013. What's the fuss over human frontal lobe evolution? Trends Cogn Sci. 17:432–433.

Shinn M, Romero-Garcia R, Seidlitz J, Váša F, Vértes PE, Bullmore E. 2017. Versatility of nodal affiliation to communities. Sci Rep. 7:4273.

Sinclair B, Hansell NK, Blokland GAM, Martin NG, Thompson PM, Breakspear M, de Zubicaray GI, Wright MJ, McMahon KL. 2015. Heritability of the network architecture of intrinsic brain functional connectivity. Neuroimage. 121:243–252.

Smaers JB, Gómez-Robles A, Parks AN, Sherwood CC. 2017. Exceptional evolutionary expansion of prefrontal cortex in great apes and humans. Curr Biol. 27:714–720.

Smith SM, Vidaurre D, Beckmann CF, Glasser MF, Jenkinson M, Miller KL, Nichols TE, Robinson EC, Salimi-Khorshidi G, Woolrich MW, et al. 2013. Functional connectomics from resting-state fMRI. Trends Cogn Sci. 17:666–682.

Sneve MH, Grydeland H, Nyberg L, Bowles B, Amlien IK, Langnes E, Walhovd KB, Fjell AM. 2015. Mechanisms underlying encoding of short-lived versus durable episodic memories. J Neurosci. 35:5202–5212.

Sporns O, Betzel RF. 2016. Modular brain networks. Annu Rev Psychol. 67:613–640. 67:annurev-psych- 122414-033634.

Tagliazucchi E, Laufs H. 2014. Decoding wakefulness levels from typical fMRI resting-state data reveals reliable drifts between wakefulness and sleep. Neuron. 82:695–708.

Toro R, Perron M, Pike B, Richer L, Veillette S, Pausova Z, Paus T. 2008. Brain size and folding of the human cerebral cortex. Cereb Cortex. 18:2352–2357.

van den Heuvel MP, Stam CJ, Kahn RS, Hulshoff Pol HE. 2009. Efficiency of functional brain networks and intellectual performance. J Neurosci. 29:7619–7624.

van den Heuvel MP, van Soelen ILC, Stam CJ, Kahn RS, Boomsma DI, Hulshoff Pol HE. 2013. Genetic control of functional brain network efficiency in children. Eur Neuropsychopharmacol. 23:19–23.

Van Essen DC, Drury HA, Dickson J, Harwell J, Hanlon D, Anderson CH. 2001. An integrated software suite for surface-based analyses of cerebral cortex. J Am Med Inform Assoc. 8:443–459.

van Kesteren MTR, Fernández G, Norris DG, Hermans EJ. 2010. Persistent schema-dependent hippocampal-neocortical connectivity during memory encoding and postencoding rest in humans. Proc Natl Acad Sci USA. 107:7550–7555.

Vendetti MS, Bunge SA. 2014. Evolutionary and developmental changes in the lateral frontoparietal network: a little goes a long way for higher-level cognition. Neuron. 84:906–917.

Vincent JL, Patel GH, Fox MD, Snyder AZ, Baker JT, Van Essen DC, Zempel JM, Snyder LH, Corbetta M, Raichle ME. 2007. Intrinsic functional architecture in the anaesthetized monkey brain. Nature. 447:83–86.

Vuoksimaa E, Panizzon MS, Chen CH, Fiecas M, Eyler LT, Fennema-Notestine C, Hagler DJ, Franz CE, Jak AJ, Lyons MJ, et al. 2016. Is bigger always better? The importance of cortical configuration with respect to cognitive ability. Neuroimage. 129:356–366.

Walhovd KB, Fjell AM, Giedd J, Dale AM, Brown TT. 2016. Through thick and thin: a need to reconcile contradictory results on trajectories in human cortical development. Cereb Cortex. 1989:bhv301.

Wang D, Buckner RL, Fox MD, Holt DJ, Holmes AJ, Stoecklein S, Langs G, Pan R, Qian T, Li K, et al. 2015. Parcellating cortical functional networks in individuals. Nat Neurosci. 18: 1853–1860.

Wechsler D. 1999. Wechsler Abbreviated Scale of intelligence. San Antonio, TX: The Psychological Corporation.

Woodward A, Hashikawa T, Maeda M, Kaneko T, Hikishima K, Iriki A, Okano H, Yamaguchi Y. 2018. Data descriptor: the brain/MINDS 3D digital marmoset brain atlas. Sci Data. 5:1–12.

Yeo BTT, Krienen FM, Eickhoff SB, Yaakub SN, Fox PT, Buckner RL, Asplund CL, Chee MWLL. 2015. Functional specialization and flexibility in human association cortex. Cereb Cortex. 25:3654–3672.

Yeo BTT, Krienen FM, Sepulcre J, Sabuncu MR, Lashkari D, Hollinshead M, Roffman JL, Smoller JW, Zöllei L, Polimeni JR, et al. 2011. The organization of the human cerebral cortex estimated by intrinsic functional connectivity. J Neurophysiol. 106:1125–1165.